

Selection Rule for Electromagnetic Transitions in Nuclear Chiral Geometry

Ikuko Hamamoto^{1,2}

¹ *Division of Mathematical Physics,
Lund Institute of Technology at the University of Lund,
Lund, Sweden*

² *The Niels Bohr Institute,
Blegdamsvej 17, Copenhagen Ø,
DK-2100, Denmark*

Abstract

In order to find the selection rules that can be applied to the electromagnetic transitions when the chiral geometry is achieved, a model for a special configuration in triaxial odd-odd nuclei is constructed which exhibits degenerate chiral bands with a sizable rotation. A quantum number obtained from the invariance of the Hamiltonian is given and the selection rule for electromagnetic transition probabilities in chiral bands is derived in terms of this quantum number. Among the available candidates for chiral bands of odd-odd nuclei, in which the near degeneracy of two $\Delta I = 1$ bands is observed, the measured electromagnetic properties of the two bands in $^{128}_{55}\text{Cs}_{73}$ and $^{126}_{55}\text{Cs}_{71}$ are consistent with the rules, while those of $^{134}_{59}\text{Pr}_{75}$ and $^{132}_{57}\text{La}_{75}$ are not.

PACS numbers: 21.10.Re,21.10.Ky,21.60.Ev,27.60.+j

I. INTRODUCTION

The possible occurrence of chirality in nuclear structure was pointed out more than ten years ago [1]. Since then, the observation of two almost degenerate $\Delta I=1$ bands possibly with the same parity has been reported, especially in the $A \approx 130$ odd-odd nuclei. Though the observed near degeneracy of the two bands is a primary indication of chiral geometry, this geometry can be pinned down in a more definitive way if electromagnetic transition probabilities expected for the chiral bands are experimentally confirmed.

Chirality in triaxial nuclei is characterized by the presence of three angular-momentum vectors, which are generally noncoplanar and thereby make it possible to define chirality. An example is shown in Fig. 1a. When chiral geometry is realized, observed two chiral-degenerate states are written as

$$\begin{aligned} |I+\rangle &= \frac{1}{\sqrt{2}} (|IL\rangle_+ |IR\rangle) \\ |I-\rangle &= \frac{i}{\sqrt{2}} (|IL\rangle_- |IR\rangle) \end{aligned} \quad (1)$$

where left- and right-handed geometry states are written as $|IL\rangle$ and $|IR\rangle$, respectively. If there were no tunneling between the R and L systems, the energies of the states associated with opposite handedness would be degenerate and one obtains

$$\langle IL | E2 | IR \rangle \approx 0 \quad \text{and} \quad \langle IL | M1 | IR \rangle \approx 0$$

for states with $I \gg 1$, where the electric-quadrupole and magnetic-dipole operators are denoted by $E2$ and $M1$, respectively. If \approx in the above expressions is replaced by $=$, two intra-bands or inter-bands transitions or two static moments, which correspond to each other within the observed pair of chiral bands, are equal. The correspondence is illustrated in Fig. 1b. This is a trivial and straightforward rule in the case of the ideal chiral bands. However, we want to take one step further with the selection rules.

II. MODEL, QUANTUM NUMBER AND SELECTION RULE

A limiting case of the particle-rotor model is considered which may be applicable to the majority of odd-odd nuclei, in which the observation of the near degeneracy of two $\Delta I = 1$

bands has so far been reported¹. In our opinion an application of this special theoretical limit outweighs a loss of generality.

The model consists of a triaxially deformed core with $\gamma = 90^\circ$ coupled to one proton particle and one neutron hole in the same single- j -shell.² Taking the long, short, and intermediate axes of the triaxial body as the 1-, 2- and 3-axes, the rotational Hamiltonian of the core is written as

$$H_{rot} = \frac{\hbar^2}{8\mathfrak{I}_0} [R_3^2 + 4(R_1^2 + R_2^2)] \quad (2)$$

where \vec{R} expresses the core angular momentum and the γ -dependence of the hydrodynamical moments of inertia is assumed. The γ -dependence is approximately supported also by microscopic numerical calculations of moments of inertia. In the case of a single- j -shell configuration the triaxially quadrupole deformed potential can be written for $\gamma = 90^\circ$ as [3]

$$V_{sp}^\pi \propto (j_{p1}^2 - j_{p2}^2) \quad (3)$$

for the proton particle and as

$$V_{sp}^\nu \propto (j_{n2}^2 - j_{n1}^2) \quad (4)$$

for the neutron hole, using the fact that the one-particle matrix-elements of $(Y_{22} + Y_{2-2})$ are proportional to those of $(j_1^2 - j_2^2)$. In Eqs. (3) and (4) j_{p1} and j_{p2} (j_{n1} and j_{n2}) denote the components of the proton (neutron) angular-momentum operator \vec{j}_p (\vec{j}_n) along the 1- and 2- axes, respectively. The proportionality constants in (3) and (4), which are linear in the quadrupole deformation parameter β , are positive and exactly the same if protons and neutrons are in the same single- j -shell. It is noted that in respective Hamiltonians of the proton particle, the neutron hole and the core the energetically preferred directions of relevant angular momenta are

$$\vec{j}_p // \pm 2\text{-axis}, \quad \vec{j}_n // \pm 1\text{-axis}, \quad \text{and} \quad \vec{R} // \pm 3\text{-axis}.$$

However, one must look for the energy minimum for a given total angular momentum I where $\vec{I} = \vec{R} + \vec{j}_p + \vec{j}_n$. Thus, the relative direction between the three vectors depends on the magnitude of I . (See Fig. 3.)

¹ The contents of the present section are based on the work published in Ref. [2].

² The "rotation with $\gamma = 90^\circ$ " is equivalent to the " $\gamma = -30^\circ$ rotation" in the Lund convention except that the intermediate axis is the quantization axis (taken to be the 3-axis).

The total particle-rotor Hamiltonian constructed from (2), (3) and (4) has the following properties.

(i) D_2 symmetry [4], which leads to $R_3 = 0, \pm 2, \pm 4, \dots$

(ii) Invariance under the operation A which consists of: (a) a rotation $exp(i(\pi/2)R_3)$ or $exp(i(3\pi/2)R_3)$, combined with (b) an exchange of valence proton and neutron.

Denoting the operator that exchanges valence proton and valence neutron by C , we assign the values $C = +1$ and $C = -1$ to the components of the intrinsic neutron-proton wave functions which are symmetric and antisymmetric under the operation C , respectively. Eigenstates of the total Hamiltonian have a quantum number $A = \pm 1$, irrespective of whether the chiral geometry is achieved or not. The possible combinations of R_3 and C for a given value of A are shown in Table 1.

For E2 transitions we take into account only the collective part, namely only the core contribution. Then, in order to obtain non-zero $B(E2)$ values, we must have both $\Delta C = 0$ and $\Delta R_3 \neq 0$. The former is required since the neutron and proton are spectators under the E2 transitions, while the latter is required since E2 matrix elements with $\Delta R_3 = 0$ vanish for the shape of $\gamma = 90^\circ$. Since the E2 operator can make only $|\Delta R_3| \leq 2$, the above condition of both $\Delta C = 0$ and $\Delta R_3 \neq 0$ leads to

$$\Delta A \neq 0 \quad \text{in order to have} \quad B(E2) \neq 0 \quad (5)$$

when we examine the contents of the eigenstates with a given A value shown in Table 1.

The M1 transition operator in the particle-rotor model is written as [4]

$$(M1)_\mu = \sqrt{\frac{3}{4\pi}} \frac{e\hbar}{2mc} \left((g_\ell - g_R) \ell_\mu + (g_s^{eff} - g_R) s_\mu \right) \quad (6)$$

If we take, for example, $g_\ell = g_\ell^{free}$ and $g_s^{eff} = 0.6 g_s^{free}$ and $g_R = 0.5$, we obtain

$$\begin{array}{lll} g_\ell - g_R = 0.5 & g_s^{eff} - g_R = 2.848 & \text{for protons} \\ g_\ell - g_R = -0.5 & g_s^{eff} - g_R = -2.792 & \text{for neutrons} \end{array}$$

Then, we obtain $B(M1) \approx 0$ for $\Delta C = 0$, since the M1 operator is almost antisymmetric under the exchange of valence proton and valence neutron. Since the M1 operator can make only $|\Delta R_3| \leq 1$, we obtain

$$[B(M1) \text{ with } \Delta A \neq 0] \gg [B(M1) \text{ with } \Delta A = 0] \quad (7)$$

examining the contents of eigenstates with a given A value in Table 1.

The static quadrupole moment of a triaxially deformed core with $\gamma = 90^\circ$ vanishes. On the other hand, the static magnetic moment in the present model is not negligible, since the magnetic moment operator can be written as

$$\vec{\mu} = g_R \vec{R} + g_\ell \vec{\ell} + g_s \vec{s} = g_R \vec{I} + (g_\ell - g_R) \vec{\ell} + (g_s - g_R) \vec{s} \quad (8)$$

and has an extra term $g_R \vec{I}$ compared with the M1 transition operator in (6).

In the present model with the chiral geometry the exchange of the right-handed with left-handed systems can be equally obtained by the exchange of the valence proton and neutron while keeping the direction of \vec{R} unchanged; see Fig. 1a. Since the rotation about the 3-axis, $\exp(i(\pi/2)R_3)$ or $\exp(i(3\pi/2)R_3)$, does not affect chirality, the operation A exchanges $|IR\rangle$ with $|IL\rangle$,

$$A|IL\rangle \propto |IR\rangle \quad \text{and} \quad A|IR\rangle \propto |IL\rangle$$

Then, the formation of chirality means that the two nearly degenerate states $|I+\rangle$ and $|I-\rangle$ have different eigenvalues of A

$$A|I+\rangle = \pm |I+\rangle \quad \Leftrightarrow \quad A|I-\rangle = \mp |I-\rangle \quad (9)$$

Now, when bands are, by definition, arranged so that $\Delta I = 2$ E2 transitions are enhanced and always allowed within respective bands, the sign of A in a given band must change at every increase of I by 2, as illustrated in Fig. 2a. And, from the arguments described in the previous paragraphs the quantum number A of the final state must have a different sign from that of the initial state, in order to have strong $E2$ or $M1$ transitions. The consequence of the present selection rules with chiral geometry is illustrated in Fig. 2a.

We have chosen the particle-rotor Hamiltonian so that if at all possible the chiral geometry may easily appear at moderate values of I . So, next, we try to numerically diagonalize our particle-rotor Hamiltonian, taking $j = h_{11/2}$ for both valence neutron and valence proton. In order to simulate a possible chiral nucleus in the mass $A \approx 130$ region, the parameters $A=130$, $Z=55$, $\beta=0.3$, and $\mathfrak{S}_0=8.55 \text{ } \hbar^2/\text{MeV}$ are used. The results of the diagonalization are shown in Fig.2b. For $13 < I < 24$ the approximate degeneracy of the two lowest bands, which are indicated by f and u , is a good sign of the realization of chiral geometry. The bands in Fig. 2b are organized based on energy at low spins close to the band-heads, while

they are based on $B(E2; I \rightarrow I - 2)$ values over the degenerate spin range which is indicated by a box. The characteristic features of electromagnetic transitions, which are expected for the chiral geometry as illustrated in Fig. 2a, are produced exactly in the transitions between the states inside the box of Fig. 2b.

The relation between three angular momentum vectors, \vec{R} , \vec{j}_p and \vec{j}_n , in the lowest-lying states for a given I is illustrated in Fig. 3. At small rotation it is energetically cheaper for the vector \vec{R} to be placed on the plane which is specified by \vec{j}_p and \vec{j}_n , when a given value of I has to be constructed. See the left figure of Fig. 3. On the other hand, since at very high spins the rotational energy becomes dominant, \vec{R} points to the direction of the 3-axis to save the energy, and both \vec{j}_p and \vec{j}_n start to rotationally align also in the direction of the 3-axis. See the right figure of Fig. 3. Consequently, only at moderate rotation the chiral geometry may be expected. This is what is seen in the calculated level scheme and transitions shown in Fig. 2b.

It is noted that the invariance of the total Hamiltonian and the selection rule for electromagnetic transitions described above also apply in the presence of pair correlation that is treated in the BCS approximation.

III. COMPARISON WITH EXPERIMENTAL DATA AND PERSPECTIVES

There are a series of odd-odd nuclei in the $A \approx 130$ region [7], in which the energies of two $\Delta I = 1$ rotational bands are observed to be roughly degenerate (namely, up till a few hundreds keV energy difference), though in fact the equality of spin-parity has hardly been experimentally proved in any of those nearly degenerate states. Up till several years ago the observed nearly degenerate pair-bands in ^{134}Pr were indeed supposed to be the best example of chiral pair bands. However, the observed $B(E2; I \rightarrow I - 2)$ values of two intra-band transitions, which should be equal in the case of chiral pair bands, turned out to be different at least by a factor of two [5, 6]. Moreover, measured $M1$ transitions strongly violated the selection rule [2] described in the present paper. Thus, the pair bands in ^{134}Pr are no longer supposed to be an example of chiral pair bands. However, if so, one may ask; if the observed bands in ^{134}Pr are not the chiral pair bands, what are they? This is an even more interesting question.

Among the odd-odd nuclei in the $A \approx 130$ region there are at present two nuclei, ^{128}Cs

and ^{126}Cs , in which not only the pair bands are nearly degenerate but also the measured electromagnetic transitions [8, 9] seem to be in agreement with the present selection rule.

Deviations of the actual situation in nuclei from the simple assumption made in the present model may modify the selection rule described in the present paper. Nevertheless, the present selection rule should serve as a starting point for the study of more complicated nuclear systems. In this connection the confirmation of chiral geometry in odd- A nuclei such as Nd isotopes, in which \vec{j}_p in the present model is replaced by the rotationally-aligned angular momentum of the S-band, is strongly wanted. Thus, the selection rule for electromagnetic transitions in that kind of chiral geometry in odd- A nuclei should be worked out so that it can be used for examining available experimental data.

-
- [1] S. Frauendorf and J. Meng, *Nucl. Phys.* **A617** (1997) 131.
 - [2] T. Koike, K. Starosta and I. Hamamoto, *Phys. Rev. Lett.* **93** (2004) 172502.
 - [3] I. Hamamoto and B. Mottelson, *Phys. Lett. B* **127** (1983) 281; **132** (1983) 7.
 - [4] A. Bohr and B. R. Mottelson, *Nuclear Structure* (Benjamin, Reading, Massachusetts, 1975), Vol.II.
 - [5] F. Tonev *et al.*, *Phys. Rev. C* **76** (2007) 044313.
 - [6] C. Petrache, G. B. Hagemann, I. Hamamoto and K. Starosta, *Phys. Rev. Lett.* **96** (2006) 112502.
 - [7] K. Starosta *et al.*, *Phys. Rev. Lett.* **86** (2001) 971; K. Starosta, a talk given in the present workshop and the references quoted therein.
 - [8] E. Grodner *et al.*, *Phys. Rev. Lett.* **97** (2006) 172501.
 - [9] E. Grodner, a talk given in the present workshop and E. Grodner *et al.*, to be published.

TABLE I: Possible combinations of the R_3 and C values for a given value of A , noting that the present particle-rotor Hamiltonian is invariant under the operation A .

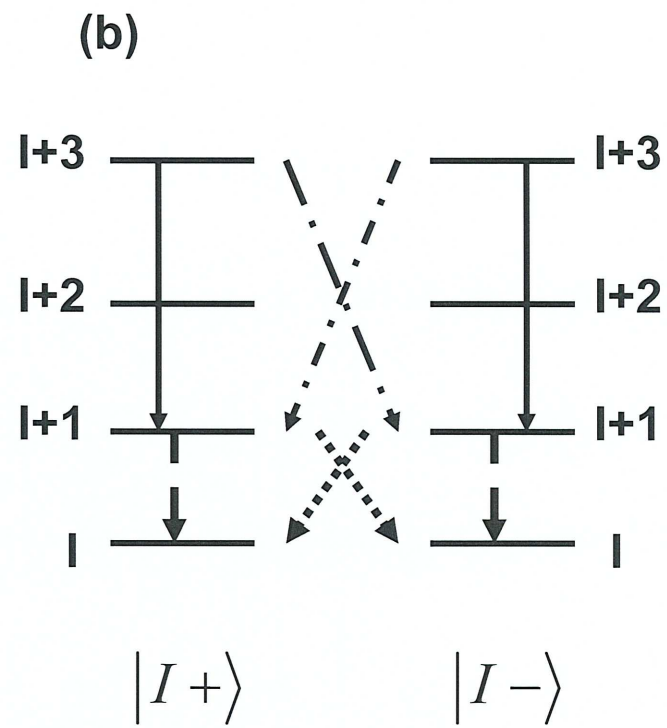
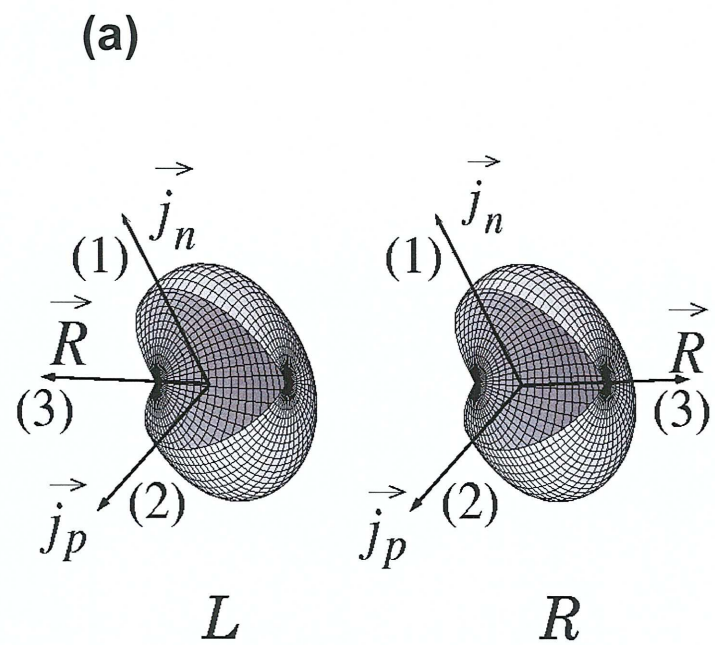
quantum-number A	R_3	C
+1	$0, \pm 4, \pm 8, \dots$	+1
	$\pm 2, \pm 6, \dots$	-1
-1	$0, \pm 4, \pm 8, \dots$	-1
	$\pm 2, \pm 6, \dots$	+1

Figure captions

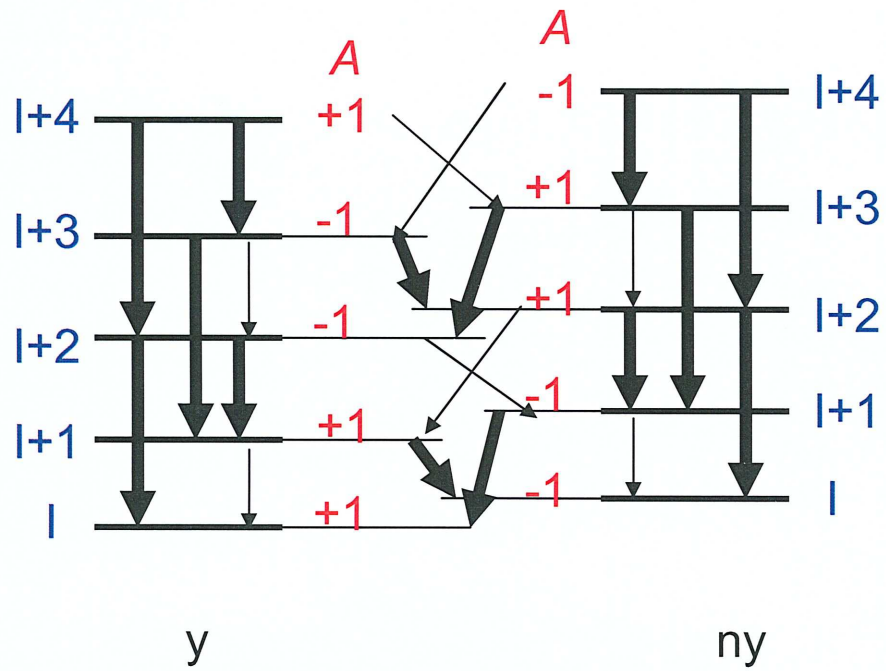
Figure 1 : (a) Sketch of the idealized chiral geometry. The core, proton, and neutron angular momenta denoted by \vec{R} , \vec{j}_p and \vec{j}_n , respectively, are parallel to the principal axes of the triaxial body, which are labeled by the numbers inside parentheses. The right-handed system is denoted by R , while the left-handed one by L . (b) In the ideal chiral geometry two transitions denoted by solid, dashed, dotted and dot-dashed lines, respectively, are equal for $I \gg 1$ and in the absence of tunneling between the L and R systems.

Figure 2 : (a) Illustration of the selection rule for inter-bands and intra-bands $E2$ and $M1$ transitions in the chiral pair bands of the present model. The yrast band denoted by "y" and the yrare bands indicated by "ny" are slightly shifted in the figure, so as to simulate practical examples. Allowed $E2$ transitions (with $\Delta I = 1$ and 2) and stronger $M1$ transitions (with $\Delta I = 1$) are indicated by thick arrows. For $\Delta I = 1$ transitions the allowed $E2$ transitions occur together with stronger $M1$ transitions, since both types of transition need a change of A quantum-number. Allowed but much weaker $\Delta I = 1$ $M1$ transitions are denoted by thinner arrows. (b) Calculated level scheme and the $E2$ and $M1$ transitions in the lowest two $\Delta I = 1$ bands, which are obtained from the diagonalization of our particle-rotor Hamiltonian. Arrows express transitions of strong $B(E2)$ or $B(M1)$, while weaker $M1$ transitions in this numerical example are practically forbidden transitions, and thus are not indicated in the figure. Solid and dashed lines represent levels with $A=+1$ and -1 , respectively, or vice versa. For $E2$ transitions, only the core contribution is taken into account, while for $M1$ transitions $g_R = 55/130 = 0.423$ and $g_s^{eff} = 0.6 g_s^{free}$ are used.

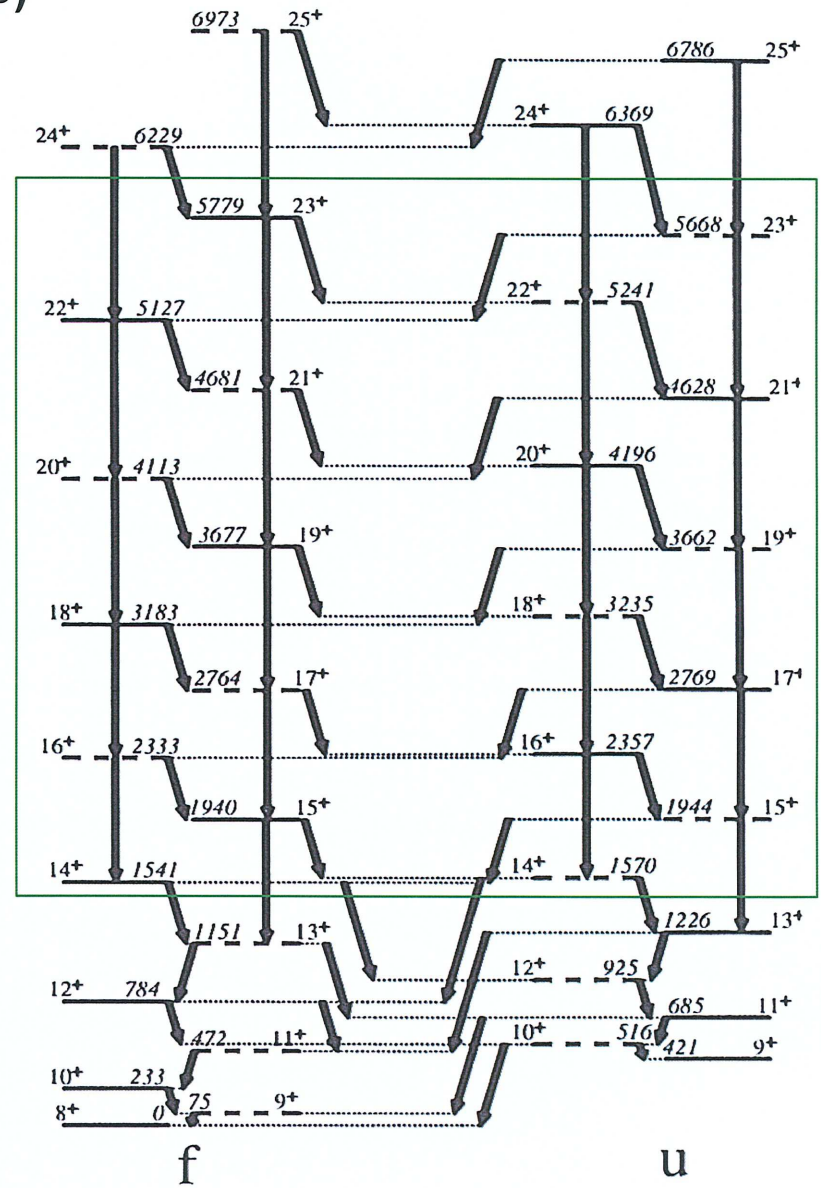
Figure 3 : The relative direction of the three angular-momentum vectors in the lowest-lying states for a given total angular momentum I , where $\vec{I} = \vec{R} + \vec{j}_p + \vec{j}_n$. In the figure \vec{j}_n and \vec{j}_p can be exchanged, for example. In respective Hamiltonians of the neutron hole, the proton particle and the core the energetically preferred directions are such that \vec{j}_n , \vec{j}_p and \vec{R} point to the ± 1 (long), ± 2 (short), and ± 3 (intermediate) axes, respectively.

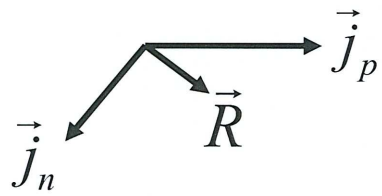


(a)

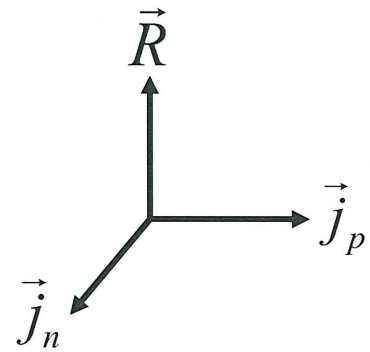


(b)

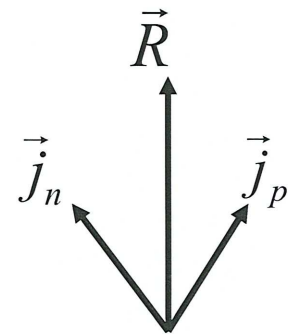




small I (small R)



Chiral geometry ?



large I (large R)